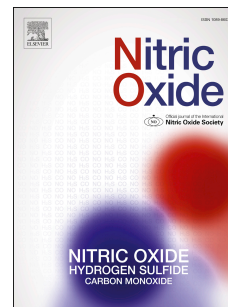


Accepted Manuscript

New generation of nitric oxide-releasing porous materials: Assessment of their potential to regulate biological functions

Rosana V. Pinto, Ana C. Fernandes, Fernando Antunes, Zhi Lin, João Rocha, João Pires, Moisés L. Pinto



PII: S1089-8603(19)30043-6

DOI: <https://doi.org/10.1016/j.niox.2019.05.010>

Reference: YNIOX 1902

To appear in: *Nitric Oxide*

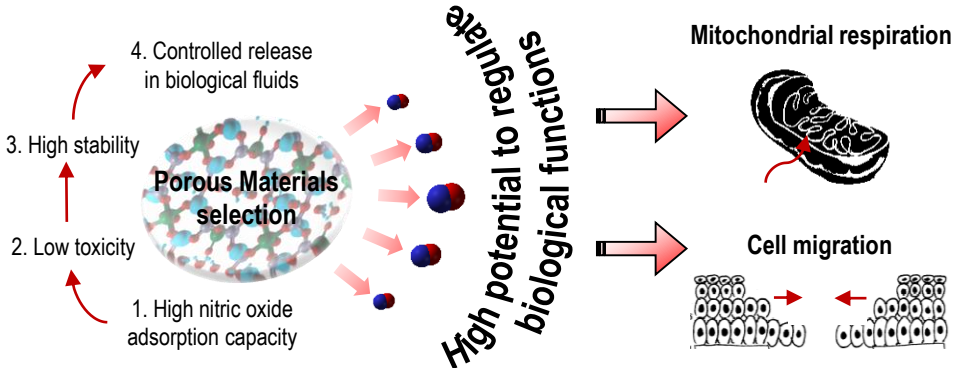
Received Date: 5 February 2019

Revised Date: 22 March 2019

Accepted Date: 28 May 2019

Please cite this article as: R.V. Pinto, A.C. Fernandes, F. Antunes, Z. Lin, Joã. Rocha, Joã. Pires, Moisés.L. Pinto, New generation of nitric oxide-releasing porous materials: Assessment of their potential to regulate biological functions, *Nitric Oxide* (2019), doi: <https://doi.org/10.1016/j.niox.2019.05.010>.

This is a PDF file of an unedited manuscript that has been accepted for publication. As a service to our customers we are providing this early version of the manuscript. The manuscript will undergo copyediting, typesetting, and review of the resulting proof before it is published in its final form. Please note that during the production process errors may be discovered which could affect the content, and all legal disclaimers that apply to the journal pertain.



1 **New generation of nitric oxide-releasing porous materials:**
2 **Assessment of their potential to regulate biological functions**

3

4 *Rosana V. Pinto,^{a,b} Ana C. Fernandes,^b Fernando Antunes,^b Zhi Lin,^c João Rocha,^c*
5 *João Pires^b and Moisés L. Pinto^{*a}*

6

7 ^a CERENA, Department of Chemical Engineering, Instituto Superior Técnico,
8 University of Lisbon, 1049-001 Lisbon, Portugal.

9 ^b CQB and CQE, Department of Chemistry and Biochemistry, Faculty of Sciences,
10 University of Lisbon, Ed. C8, Campo Grande, 1749-016 Lisbon, Portugal.

11 ^c CICECO - Aveiro Institute of Materials, Department of Chemistry, University of
12 Aveiro, Campus Universitário de Santiago, 3810-193 Aveiro, Portugal

13

14 * Corresponding author.

15 E-mail address: moises.pinto@tecnico.ulisboa.pt;

16 Address: Departamento de Engenharia Química, Instituto Superior Técnico,
17 Universidade de Lisboa; Av. Rovisco Pais, nº 1, 1049-001 Lisboa, Portugal

18

19

20

21 **Keywords:** Adsorption; Nitric Oxide; NO donors; Controlled Delivery Systems; Porous
22 Materials; Wound Healing.

23

24

25

26

27

28 **Abstract**

29

30 Nitric oxide (NO) presents innumerable biological roles, and its exogenous supplementation for

31 therapeutic purposes has become a necessity. Some nanoporous materials proved to be potential

32 vehicles for NO with high storage capacity. However, there is still a lack of information about

33 their efficiency to release controlled NO and if they are biocompatible and biologically stable.

34 In this work, we address this knowledge gap starting by evaluating the NO release and stability

35 under biological conditions and their toxicity with primary keratinocyte cells. Titanosilicates

36 (ETS-4 and ETS-10 types) and clay-based materials were the materials under study, which have

37 shown in previous studies suitable NO gas adsorption/release rates.

38 ETS-4 proved to be the most promising material, combining good biocompatibility at 180

39 $\mu\text{g/mL}$, stability and slower NO release. ETS-10 and ETAS-10 showed the best

40 biocompatibility at the same concentration and, in the case of clay-based materials, CoOS is the

41 least toxic of those tested and the one that releases the highest NO amount. The potentiality of

42 these new NO donors to regulate biological functions was assessed next by controlling the

43 mitochondrial respiration and the cell migration. NO-loaded ETS-4 regulates O_2 consumption

44 and cell migration in a dose-dependent manner. For cell migration, a biphasic effect was

45 observed in a narrow range of ETS concentration, with a stimulatory effect becoming inhibitory

46 just by doubling ETS concentration. For the other materials, no effective regulation was

47 achieved, which highlights the relevance of the new assessment presented in this work for

48 nanoporous NO carriers that will pave the way for further developments.

49

50 1. Introduction

51 The potential outcome of the controlled delivery of nitric oxide (NO) to specific biological
52 targets led to the development of new NO-carrying and releasing matrices for therapeutic
53 benefit. Among its many biological roles, NO is a strong vasodilator, antimicrobial agent and
54 wound healing accelerator, and its use as a therapeutic agent provides an excellent alternative to
55 conventional drugs [1,2]. Generically, therapy relies both on NO donors that release the
56 molecule in a direct or indirect way (*i.e.*, via metabolic activity, biotransformation or redox
57 activation), and on agents that increase NO bioactivity [3]. Most of existing molecular donors
58 present, however, certain limitations when in contact with biological fluids, namely high
59 solubility, non-target and uncontrolled NO release and the release of toxic decomposition
60 products (*e.g.* carcinogenic nitrosamines) [4–6]. For example, due to its high solubility, NO may
61 be released before reaching the target site, thus requiring higher amounts of donor to meet the
62 therapeutic needs, triggering potential toxic effects [4]. Under these circumstances, additional
63 chemical reactions become relevant, generating reactive nitrogen oxide species capable to
64 inhibit cell respiration and to induce cell toxicity [5].

65 Recent work has unveiled the NO adsorption/release potential of nanoporous framework solids
66 bearing metal active sites [3,6]. These new materials overcome the limitations of the most
67 conventional donors because they provide a safe storage and controlled delivery of pure NO in
68 the target tissue, being of special interest for topical applications [5]. In addition, the amount of
69 NO and the release period may be modulated, by tuning the porosity of the material and/or
70 varying the nature and the number of metal sites in the framework [7–9].

71 Several types of porous materials have recently been studied for this purpose, including:
72 zeolites, clays, metal-organic frameworks (MOFs) and titanosilicates [7,10–12]. We have been
73 interested in designing new porous structures for the storage and controlled release of NO. We
74 showed that microporous titanosilicates (ETS-4) containing Ti^{4+} unsaturated metal centers and
75 Cu^{2+} or Co^{2+} extra-framework cations exhibit exceptional properties to adsorb and release
76 controlled NO amounts [12,13]. Another microporous titanosilicate structure, ETS-10, and the
77 effect of its isomorphic substitution of Si by Al and Ga, was also explored [14], as well as

78 materials based on modified mineral clays (sepiolite and montmorillonite) [11,15], synthetic
79 clays (smectite clays with cobalt ions) [16] and organoclays (natural clays modified with L-
80 histidine) [17]. Clay-based materials, although storing less NO than titanosilicates and
81 displaying faster NO release still release NO amounts that may trigger positive biological
82 responses.

83 So far, studies using these new donors concerning their biocompatibility, stability and control of
84 biological processes with the NO released are still poorly explored. Only few papers, using
85 MOFs and zeolites based materials, demonstrated that NO released from those materials is able
86 to inhibit platelet aggregation [7,18], to relax smooth muscle of blood vessels [9] and stimulate
87 the wound healing process [19]. However, no actual demonstration of control of the biological
88 systems was provided, namely by establishing a relationship between the response
89 extension/intensity and the amount of NO released to the system. This is of central importance
90 to modulate the response of the biological systems at the therapeutic level and the present work
91 aims to provide this demonstration and afford a more comprehensive assessment of the real
92 potentialities of the materials.

93 The work starts by evaluating the biocompatibility using primary keratinocyte cells (HEK_n), the
94 materials' stability in biological fluids and following with the evaluation of NO release under
95 biological conditions. Materials that exhibited the best combination of good biocompatibility,
96 stability and NO slower release were then evaluated to control two relevant cellular processes:
97 (1) mitochondrial respiration and (2) cell migration, in two independent assessments. We
98 demonstrate in this work that not all materials that are able to store and release NO can be used
99 in biological systems, since they should combine several characteristics to provide a successful
100 effect.

101

102 **2. Materials and Methods**

103 **2.1. Materials**

104 ETS-4 was synthesised with an alkaline solution made by dissolving 33.16 g of meta- silicate
105 (BDH), 2.00 g NaOH (Merck), and 3.00 g KCl (Merck) into 25.40 g H₂O. 31.88 g of TiCl₃

106 (15% m/m, TiCl_3 and 10% m/m HCl, Merck) was added to this solution and stirred thoroughly.
107 This gel was transferred to a Teflon-lined autoclave and treated at 230 °C for 17 hours. The
108 product was filtered off, washed at room temperature with distilled water and dried at 70 °C
109 overnight, the final product being an off-white microcrystalline powder. This synthesis
110 optimization and product characterization are described elsewhere [20]. Cu and Co exchanged
111 ETS-4 was prepared by cation exchange with CuNO_3 and CoNO_3 solutions, and the products
112 characterized as previously described [13].
113 ETS-10, ETAS-10 and ETGS-10 were synthesized according to previously optimized
114 procedures described elsewhere [21–23], using titanium trichloride as Ti source. The materials
115 were characterized as previously described to ascertain their purity and porosity [14].
116 Sepiolite-type natural clay was obtained from the Tolsa Group, Spain. Organoclay modified
117 with L-histidine and modified synthetic clays were synthesized according to the procedures
118 previously described by Fernandes *et al.* [16,17].
119 To confirm the synthesis' purity and the solid phases obtained the materials were characterized
120 by powder X-ray diffraction (XRD) and nitrogen adsorption at -196 °C. The detailed description
121 of those experimental methods and the obtained results are in Section I of the Supplementary
122 material. All the obtained data are coincident with the literature, which ensures the purity of the
123 newly synthesized materials [11,13,16,17,20–22]. Moreover, a brief description of the materials
124 used in this study and their NO adsorption/release capacities are shown in Table 1. These
125 materials represent a selection from the studied materials by our group to date that present the
126 most promising NO storage and release properties.

127

128

129

130

131 *Table 1 – Porous materials studied in this work presenting suitable NO gas adsorption and release*
 132 *properties.*

MATERIAL	DESCRIPTION	ADSORPTION CAPACITY (%)	RELEASE CAPACITY (% m/m)	REF.
<i>ETS-10</i>	Titanosilicate with hexacoordinated framework Ti ⁴⁺	8	3	[14]
<i>ETAS-10</i>	ETS-10 with isomorphous substitution of framework Si ⁴⁺ by Al ³⁺	12	5	[14]
<i>ETGS-10</i>	ETS-10 with isomorphous substitution of framework Si ⁴⁺ by Ga ³⁺	16	2.9	[14]
<i>ETS-4</i>	Titanosilicate with unsaturated (pentacoordinated) Ti ⁴⁺	11	5	[12]
<i>Cu-ETS-4</i>	ETS-4 with extra-framework cations exchanged by Cu ²⁺	12	6.3	[13]
<i>Co-ETS-4</i>	ETS-4 with extra-framework cations exchanged by Co ²⁺	7	4	[13]
<i>Sepiolite</i>	Natural clay	1	0.6	[11]
<i>CoOS</i>	Smectite clay with Co ²⁺ in the structure using tetramethyl orthosilicate as a silicon source	5.1	2	[16]
<i>COAS-B</i>	Smectite clay with Co ²⁺ in the structure using silicic acid as a silicon source	3.5	1	[16]
<i>L-HM-1</i>	Organoclay with the modification of aluminum silicate (montmorillonite) with L-histidine	3.2	1.4	[17]

133

134

135 **2.2. NO adsorption and storage in the materials**

136 Loading of the material with NO was proceeded by introducing each sample in a glass vacuum
 137 cell with a valve and degassed under high-vacuum conditions (better than 10⁻² Pa) to activate the
 138 samples. Time and heating temperatures for degassing were different depending on the material:
 139 For ETS-4 and modified specimens, the conditions used were 100 °C for 3 h [13]; ETS-10,
 140 ETAS-10 and ETGS-10 were heated at 300 °C for 2.5 h [14]; Sepiolite was heated at 250 °C for
 141 2 h [11]; Modified organoclay with L-histidine (L-HM-1) was degassed at 150 °C for 2.5 h [17]
 142 and modified synthetic clays (CoOS and CoAS-B) at 250 °C for 2.5 h [16]. After outgassing
 143 and with the material already at room temperature, NO was admitted to the vacuum cell housing
 144 the solid, at a pressure of 80 kPa, and kept there for 3 days. After this period of NO loading, the
 145 remaining gas was evacuated by connecting the cell to the vacuum line and opening the valve.
 146 The loaded material was stored by filling immediately the valve with helium up to atmospheric
 147 pressure.

148

149

150 2.3. NO release profiles in biological media

151 NO released over time by the materials was quantified in biological medium (RPMI-1640 with
152 10% (V/V) fetal bovine serum, penicillin-streptomycin (100 UI/mL and 100 µg/mL,
153 respectively) using the method of Griess at 37 °C. This is an indirect method, which quantify its
154 decomposition product (NO₂⁻) accumulated in the medium over time [24]. After 15, 30, 60 and
155 120 minutes, 2 mL of sample with a material concentration of 450 µg / mL was centrifuged in
156 order to separate the material from the medium. Other concentrations were tested for ETS-4
157 (180, 90 and 45 µg / mL). Subsequently, the supernatant obtained after centrifugation was
158 incubated with Griess reagent (0.2% naphthylethylenediamine dihydrochloride, and 2%
159 sulphanilamide in 5% phosphoric acid) generating a chromophoric azo product, which was
160 quantified by absorbance at 548 nm, using a microplate reader (Tecan, A-5082 Sunrise
161 Remote). A calibration curve was prepared using a sodium nitrite solution (0-200 µM)
162 according to the same procedure described above for the samples.

163

164 2.4 Material's stability in biological medium

165 The material's stability in complete cellular culture medium (EpiLife® - same used for HEK293
166 cells culture) was evaluated under cell incubation conditions (37 °C, humidified atmosphere
167 with 5 % CO₂) after 72 hours (maximum time of the accomplished cellular assays), using a
168 material concentration of 450 µg/mL. Depending on the material's structure, the determination
169 of the correspondent metal(s) content in the medium was done by ICP at the laboratory of
170 analysis of Instituto Superior Técnico, following the analytical procedure defined in the
171 standard ISO 11885:2007.

172 Powder X-ray diffraction was performed using a Philips X-ray diffractometer (PW 1730) with
173 automatic data acquisition (APD Philips v3.6B), using Cu K α radiation ($\lambda = 0.15406$ nm). The
174 diffraction patterns were collected in the 2θ range of 5°–20° with a 0.01° step size and an
175 acquisition time of 200 seconds per step.

176

177

178 2.5. HeLa and HEK_n cells culture

179 HeLa cells (human cervical cancer cell line) (American Type Culture Collection, Manassas,
180 VA, USA) were cultured in supplemented RPMI-1640 with fetal bovine serum (10 % V/V),
181 penicillin-streptomycin (100 UI/mL and 100 µg/mL, respectively) and 2 mM glutamine, and
182 incubated at normal culturing conditions (37 °C, 5% CO₂). Fresh medium was replaced every 2
183 days up to adequate confluency for subcultivation.

184 HEK_n cells (epidermal keratinocytes isolated from neonatal foreskin) (Thermo Fisher
185 Scientific) were cultivated in EpiLife® Medium supplemented with 60 µM calcium, an
186 antibiotic/antimycotic solution of gentamicin and amphotericin B and an human keratinocyte
187 growth supplement (1% V/V; composed by bovine pituitary extract (0.2% V/V), recombinant
188 human insulin-like growth factor-I (1 µg/mL), hydrocortisone (0.18 µg/mL), bovine transferrin
189 (5 µg/mL) and human epidermal growth factor (0.2 ng/mL)) and an antibiotic/antimycotic
190 solution of gentamicin and amphotericin B, incubated and maintained in the conditions of HeLa
191 cells.

192

193 2.5.1 HEK_n cytotoxicity tests

194 Viability/toxicity was assessed by the fluorometric alamarBlue® assay. HEK_n cells were seeded
195 in 96-well plates at a density of 7500 or 5000 cells per well for the 24 or 72 hours experiments,
196 respectively. After 24 hours of incubation, the media were replaced by the supplemented
197 medium containing the desired concentration of the compound. Two concentrations were tested:
198 450 µg/mL and 180 µg/mL. Eight replicates were used for each condition.

199 On the respective time, 10 µL of alamarBlue® was added directly to each well and the plate
200 was incubated for at least 4 hours. alamarBlue® reduction was quantified by fluorescence ($\lambda_{\text{ex}} =$
201 530 nm, $\lambda_{\text{em}} = 590$ nm) in a Spectra Max Gemini EM reader from Molecular Devices. Cell
202 viability was calculated as follows:

$$\text{cell viability (\%)} = \frac{F_{(cells+material)}}{F_{control (cells)}} \times 100$$

203 Where $F_{(cells+material)}$ represents the average of the fluorescence obtained for the cells incubated
204 with the material and $F_{control(cells)}$ the fluorescence average of the control, which corresponds to
205 the cells incubated only with the medium. The fluorescence signal of the supplemented medium
206 was subtracted in all the conditions.

207

208 **2.5.2 Measurement of oxygen consumption rates using HeLa cells**

209 Mitochondrial respiration was measured at 37 °C using an oxygen electrode. HeLa cells (2.5 mg
210 of protein) were resuspended in 40 µL PBS, kept in ice for 5 minutes and incubated in the O₂
211 electrode chamber containing a specific respiration buffer (0.07 M sucrose, 0.23 M mannitol, 30
212 mM Tris HCl, 4 mM MgCl₂, 5 mM KH₂PO₄, 1 mM EDTA and 0.5% bovine serum albumin, pH
213 7.4) and with 0.01% digitonin (to permeabilize the cells) under stirring. Respiratory substrate
214 (20 mM succinate) was added to the mitochondrial incubation (state 4). State 3 active
215 respiration was obtained by adding ADP (0.125 mM), allowing the ATP synthase to function,
216 proton motive force to drop and electron transport to accelerate. Finally, the NO-loaded material
217 was added at the desired concentration. The following concentrations were tested: 450, 180 and
218 90 µg/mL. Respiration rates (O₂ consumption) were calculated as the negative time derivative of
219 oxygen concentration using the Oxygraph plus program. Considering the maximum respiration
220 rate reached in state 3, the mitochondrial inhibition by the NO is expressed comparatively to
221 that value. Since O₂ consumption showed some variation from day to day, the respiration rate is
222 reported as percentage of control.

223 Preliminary studies were performed without cells, by adding the different tested concentrations
224 of NO-loaded material, confirming no interference with the signal. Moreover, unloaded material
225 was also tested and no significant inhibition of the mitochondrial respiration was observed.

226

227 **2.5.3 Cell migration assay**

228 For this process, the Oris™ Cell Migration Assay (Platypus technologies, LLC, Madison WI)
229 was used by adapting the manufacturer's protocol and using HeLa cells with a confluent density
230 of 5×10^4 per well NO-loaded material was tested using different concentrations and, in
231 parallel, the unloaded material was also tested, as control. Cells were allowed to migrate into the
232 central detection zone for 48 hours. Images were captured at pre-migration time (0 hours) and
233 after 6, 12, 24 and 48 hours using a microscope (Olympus, CK40) equipped with a digital
234 camera (C4040; Olympus). For that, a black mask with 96 prefabricated openings that precisely
235 frame the central detection zone of each well, was attached to the bottom of the 96-well plate.
236 The quantification of cell migration was performed by imaging analysis using ImageJ 1.50i
237 software. All images covered the entire detection zone and the surrounding area was black due
238 to the masking plate. Using a MRI wound healing tool [25], it was possible to adjust a threshold
239 in order to obtain the value of the free area inside the detection zone that was not occupied by
240 cells. The migrated cells area at each time was calculated using the equation (1):

$$241 \quad \% \text{ cell migration or wound closure} = \frac{(Area_{pre-migration (t=0 h)} - Area_{post-migration (t=x h)})}{Area_{pre-migration (t=0 h)}} \cdot 100 \quad (1)$$

242 The average percentage of wound closure and standard deviation of the three independent
243 assays with four replicates each were reported in the results. Since, some variability is always
244 present between independent assays, the results are reported as the difference in closure
245 percentage between the control (only cells) and the cells with the new donor. Statistical analysis
246 was performed using unpaired student's t-test and the level of statistical difference was defined
247 at $p < 0.05$.

248

249 **3. Results**

250

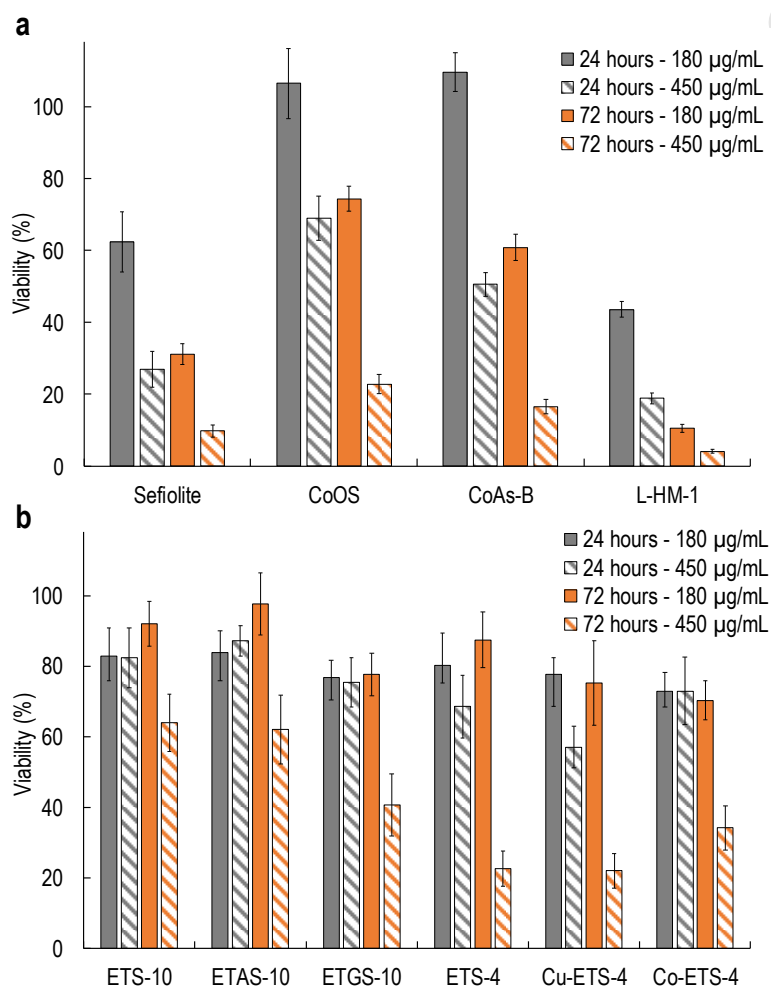
251 **3.1 HEKn biocompatibility**

252 Biocompatibility is a key for understanding the host response to a material [26]. In this context,
253 preliminary cytotoxic tests with HeLa cells have already been performed for titanosilicates
254 [13,14] and clays [11,16,17], showing very encouraging results. In order to better evaluate

255 toxicity, here we report additional tests with primary human cells. HEK_n cells were chosen due
 256 to the potential application of these materials in wound healing treatments. The obtained results
 257 are shown in Figure 1 a and b for clay-based and titanosilicate-based porous materials,
 258 respectively. Since our objective was to compare the materials and not to establish the toxicity
 259 threshold, two concentrations were tested, 180 and 450 $\mu\text{g}/\text{mL}$, the latter being at the upper limit
 260 usually used for evaluating the cytotoxicity of silicas and other porous materials [27,28] (this
 261 concentration was also used in the previous HeLa tests).

262

263



264

265 **Fig. 1 – Cytotoxicity assays with selected porous materials.** Viability results for **a)** clay-based materials and **b)**
 266 selected titanosilicates using primary keratinocytes (HEK_n) after 24 and 72 hours of incubation. All materials were
 267 tested without NO, at a concentration of 450 and 180 $\mu\text{g}/\text{mL}$, represented by striped and solid bars, respectively. The
 268 error bars represent the standard deviation of eight replicates.
 269

270 For clay-based samples (Fig. 1 a), results with the higher concentration (450 $\mu\text{g}/\text{mL}$) reflected
271 high toxicity after 72 hours, with 20% cells survival at best case (CoOS). At low concentration
272 (180 $\mu\text{g}/\text{mL}$) CoOS and CoAs-B present no toxicity after 24 hours and a survival rate of at least
273 60% after 72 hours. Since the natural clay sepiolite and L-HM-1 present toxicities higher than
274 50% after 72 hours even at low concentration, their use in biological systems is not
275 recommended.

276 The biocompatibility results of titanosilicates (Fig. 1 b) revealed a considerable toxicity at the
277 longer exposure time (72 hours) at high concentration (striped bars), which is more evident in
278 ETS-4 and ETS-4 based materials (toxicity > 70%). At low concentrations (full bars), cells'
279 survival increased significantly (75% viability for the worst case, Co-ETS-4). Additionally,
280 toxicity was assessed with selected materials loaded with NO and compared with unloaded ones
281 (Supplementary Figure A.8). Although high amounts of material have been used (450 $\mu\text{g}/\text{mL}$) in
282 both conditions, no significant differences in toxicity were observed, which indicates that the
283 concentration of NO released by these materials (450 $\mu\text{g}/\text{mL}$) is not enough to induce toxicity.

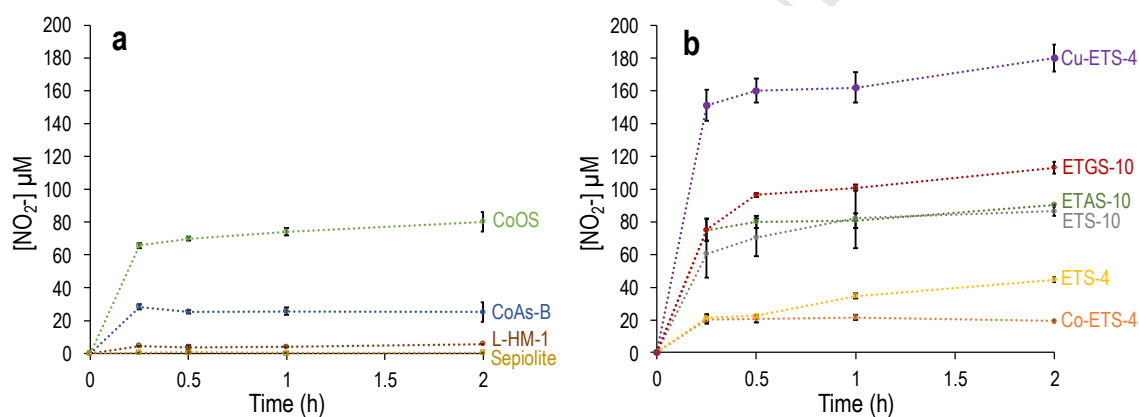
284 Overall, results demonstrated an increased susceptibility when using primary cells, comparing
285 with the results obtained with HeLa cells [11,13,14,16,17]. For instance, HeLa cells in contact
286 with sepiolite at 450 $\mu\text{g}/\text{mL}$ presented $\sim 70\%$ cell survival after 72 h [11], in clear contrast with
287 the $\sim 10\%$ cell survival observed with HEK293 cells in the present work (Fig. 1). Comparing with
288 other porous materials studied for this purpose, for instance vitamin B₃ MOFs with Ni and Co
289 metal centres [10], both MOFs present toxicities higher than 60% at 450 $\mu\text{g} / \text{mL}$ after 72 h in
290 contact with the same cell line. This toxicity is comparable with the results presented here (Fig.
291 1 and 2) for most of the materials. Tests of common zeolites carried out with various cell lines
292 [7,18] show that those materials are less toxic (20% at high concentration) than most materials
293 assessed in this work [34–36]. However, zeolites present lower NO adsorption/release capacity.

294

295 **3.2 NO release and materials' stability in biological media**

296 Having knowledge about the NO release behaviour of these materials under biological
297 environments is also extremely important for developing useful therapeutics, since beneficial

298 effects of any NO-based drug depend strongly on the concentration and duration of the NO
 299 delivery [29]. Previous studies of NO release kinetics in liquid phase relied on the
 300 oxyhemoglobin assay [30], using a haemoglobin solution at room temperature [12]. However,
 301 for a more consistent evaluation, the physiological medium used should mimic closely that of
 302 the proposed application. For example, the amount of available NO released from a material in
 303 blood is significantly lower than in phosphate buffered saline solution [31]. Thus, NO release
 304 studies were performed in the present work using the Griess reagent assay under *in vitro*
 305 biological conditions.
 306 Figure 2 a) and b) displays the NO release profiles obtained for titanosilicates and clays,
 307 respectively.



308

309 **Fig. 2 – Nitric oxide release studies under biological conditions.** Concentration of nitrite measured by Griess
 310 reagent assay in supplemented RPMI-1640 medium in the presence of NO-loaded materials at a concentration of 450
 311 $\mu g/mL$: a) release profiles from the selected modified titanosilicates and b) release profiles from the selected
 312 modified clays. All the measurements were performed at 37 °C. The error bars represent the standard deviation of
 313 three assays.

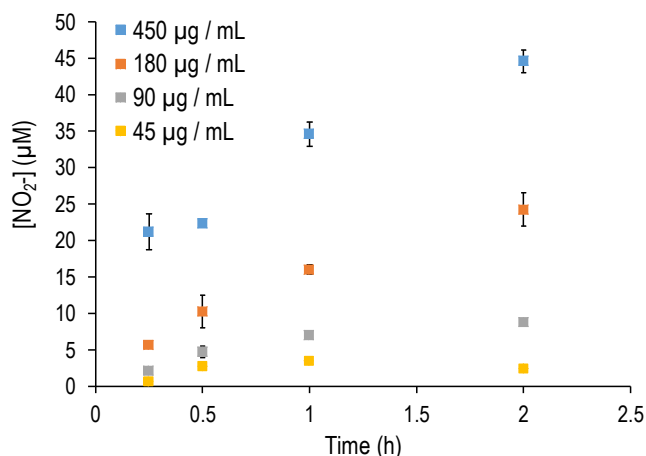
314

315 On the overall, titanosilicates release higher amounts of NO than clays, with exception to the
 316 CoOS which presented a release within the range of the titanosilicates. In three specific cases,
 317 ETS-4, ETGS-10 and Cu-ETS-4, the release can be controlled over time as shown by the slow
 318 increase of nitrite in the solution, particularly in the ETS-4 case. For this material, the NO
 319 released amount increased almost linearly with time, which is the most favourable release
 320 kinetic for drug delivery systems [32]. Although ETS-4 was not the material that releases the
 321 highest amount of NO, it ensures that no exaggerated amounts of NO are released in the first
 322 few minutes, since this effect may induce toxicological effects on the surrounding tissues. The

323 highest nitrite release at 450 $\mu\text{g/mL}$ was achieved by Cu-ETS-4 (up to 180 μM), with the
324 highest amount of NO being released in the first few minutes. Similarly, a fast (up to 15
325 minutes) NO release is observed from ETS-10 and related materials (ETAS-10 and ETGS-10),
326 which may be limiting for future therapeutic applications.

327 Regarding clay-based materials, L-HM-1 and Sepiolite do not release any significant amounts
328 of NO, whereas CoOS is the most promising material (80 μM nitrite after 2 hours), but this
329 release is very fast which may limit its applicability.

330 Overall, titanosilicates clearly released higher amounts, as was previously demonstrated through
331 NO adsorption/desorption studies of each material (Table 1). Although the adsorbed NO is
332 never fully released under vacuum, it was possible to confirm the higher capacity of adsorption
333 and release of titanosilicates [11–14,16,17]. These NO release results are not easily comparable
334 to those described in the literature for nanoporous solids designed for the same purpose since
335 different media, concentrations and temperature conditions were used. For instance, release
336 studies of Zn^{2+} -exchanged zeolite carried out with a NO electrode, in 5% LB:PBS media and at
337 37 $^{\circ}\text{C}$, revealed significant NO flow in the first 10 minutes that decreased to near zero thereafter
338 [37]. Nevertheless, such burst efficiently inhibited bacterial growth [37]. The more sustained
339 NO release profile obtained for ETS-4 prompted us to study its release profile at lower
340 concentrations (Figure 3), since at 450 $\mu\text{g/mL}$ some toxicity is noticed (Fig. 1 b). These results
341 demonstrated a time-dependent and concentration-dependent NO release over 2 hours. This
342 supports the high potential of applying this compound to achieve a control release of NO
343 concentrations that is essential for pharmacological applications.



344

345 **Fig. 3– Indirect nitric oxide release studies of ETS-4 at different concentrations under biological conditions.**
 346 Nitrite release levels from NO loaded ETS-4 were measured in RPMI-1640 medium at 37 °C, using Griess reagent.
 347 The error bars represent the standard deviation of eight assays.

348

349 Materials' stability is also another requirement for a successful NO carrier, being critical to
 350 ensure the storage of the gas, its controlled release and to avoid the leaching of their
 351 components in the tissues that may cause potential side reactions. Thus, the stability of the
 352 present materials under biological conditions was tested and the respective data are shown in
 353 Supplementary Table A.2. Except for Cu-ETS-4 and Co-ETS-4, titanosilicates present excellent
 354 stability in HEK293 cell culture by showing no release of metals to the medium, which is
 355 indicative of absence of degradation by the materials. Cu-ETS-4 and Co-ETS-4 assays,
 356 however, present a Cu²⁺ and Co²⁺ concentrations of 21.25 and 4.25 μg/mL, respectively, in the
 357 culture medium, indicating that these exchangeable cations that compensate the charge of the
 358 framework can be released/exchanged when in contact with cell culture medium. In the case of
 359 clay-based materials, all exhibit some degradation proved by considerable amounts of the
 360 correspondent metals detected in the medium.

361 To confirm overall results, a more comprehensive study with XRD was performed with one of
 362 those materials, namely ETS-4, by comparing its XRD pattern before and after submersion in
 363 the biological medium for 72 hours (Supplementary Figure A.9). The results did not present any
 364 significant changes in the material's crystallinity, which confirm its stability. Although the

365 amount of free metals in the medium is not the only aspect that drives toxicity, overall stability
366 results (Supplementary Table A.2) are in line with the toxicity tests (Fig. 1).

367

368 **3.3 Biological effects of NO-loaded materials**

369 **3.3.1 Mitochondrial respiration**

370 To establish this new class of NO donors as a viable alternative in the control of biological
371 functions, the impact of the active NO released on the biological systems must be addressed.

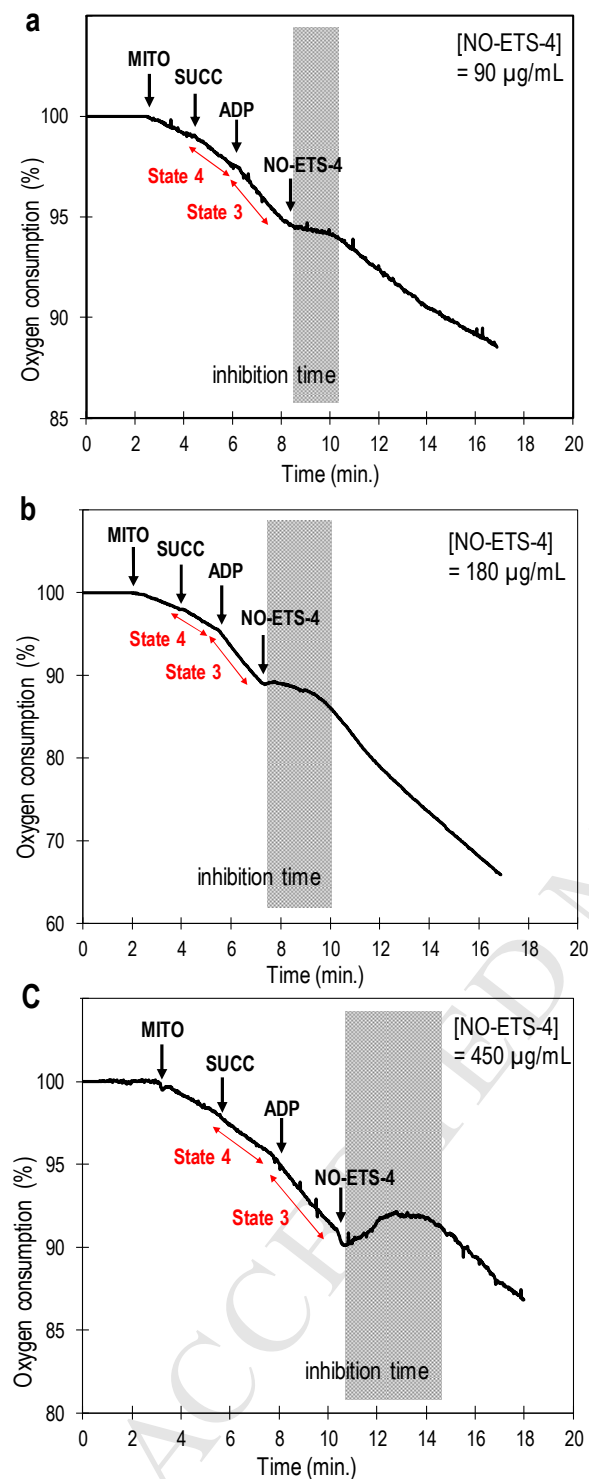
372 Thus, effects on the mitochondrial respiration were evaluated by measuring the oxygen
373 consumption of digitonin-permeabilized HeLa cells exposed to NO-loaded ETS-4 using a O₂
374 electrochemical sensor. Figure 4 displays the variances in the O₂ consumption profiles by
375 exposing the cells to different concentrations of NO-loaded ETS-4 (90, 180 and 450 µg/mL).

376 Using the lower NO donor concentration (Fig. 4 a), the mitochondrial oxygen consumption was
377 reversibly inhibited by the material, attaining an inhibition maximum of 76.7±2.4% and
378 returning to normal values after ~2 minutes as the NO concentration decayed. For a higher
379 ETS-4 concentration (180 µg/mL, Fig. 4 b), the inhibition of the respiration rate was similar

380 (73.4±1.7%) but was observed for a longer period (~2.6 minutes). For 450 µg/mL of NO-
381 loaded ETS-4 (Fig.4 c), an abrupt decrease in the oxygen consumption was observed for an
382 even longer period (~4 minutes) caused by higher release of active NO to the medium.

383 Calculation of oxygen consumption inhibition was not possible due to interferences in the O₂
384 signal caused by the high amount of solid in the suspension. Overall, the main variation
385 observed by changing the concentration was the duration of respiration inhibition that increased
386 with the amount of NO released, highlighting the high dependence of the NO concentration in
387 the control of the biological effect.

388



389

390 **Fig. 4 – Impact of NO released from ETS-4 in oxygen cell consumption.** O_2 consumption profiles of digitonin-
 391 permeabilized cells (1.25 mg of protein) exposed to different concentrations of NO-loaded ETS-4: **a)** 90 µg/mL; **b)**
 392 180 µg/mL and **c)** 450 µg/mL. The material was added after reaching the state 3 respiratory conditions, defined by
 393 the state of maximal phosphorylation after the addition of ADP.

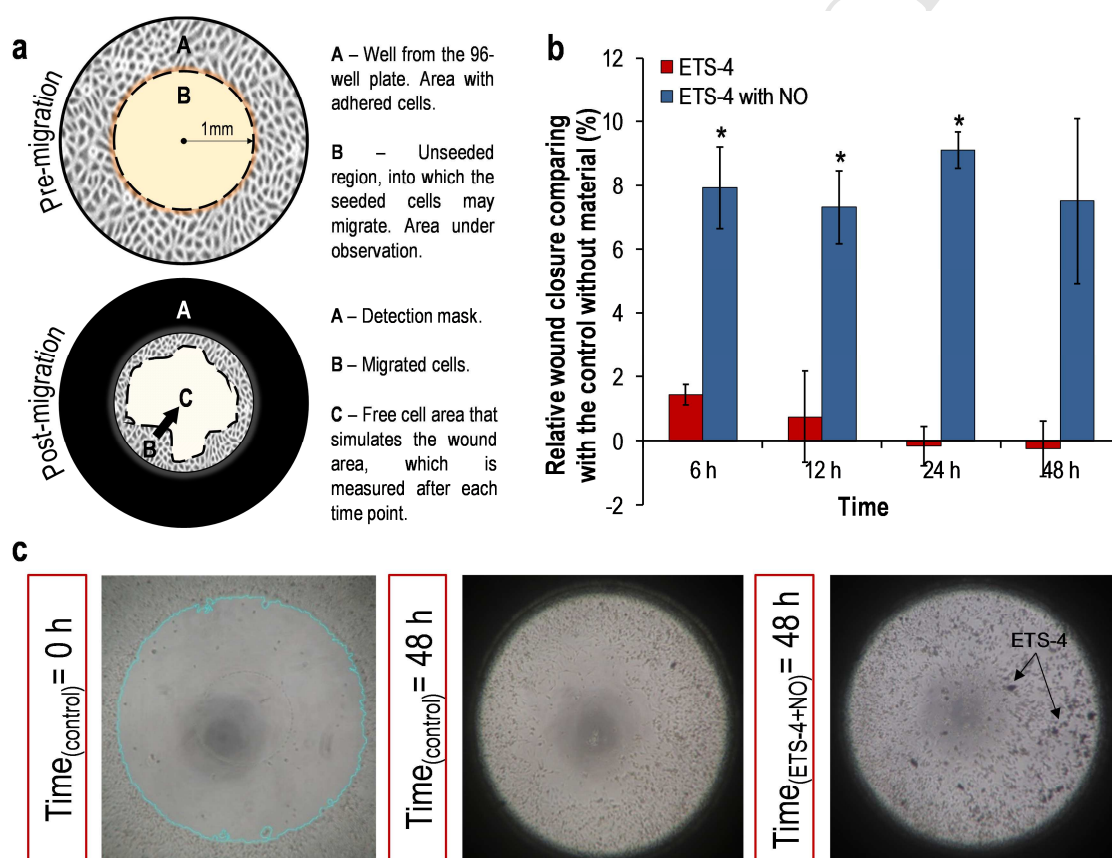
394

395

396 **3.3.2 Cell migration**

397 To evaluate the efficiency of the released NO from the new donors in wound therapy, in vitro
 398 models were created. Cell migration was then evaluated using Oris™ Cell Migration Assay,
 399 with the conditions optimized for this type of solid NO carriers, with HeLa cells. This cell line
 400 was used as a starting point for these tests due to its fast growth and easy maintenance, which
 401 allows the observation of results within a few days. Figure 5a illustrates the schematic
 402 representation of the migration assay.

403



404

405 **Fig. 5 – Enhancement of cell migration and proliferation during Oris™ cell migration assay with NO-loaded**
 406 **ETS-4 using HeLa cells.** **a**) Scheme showing Oris™ cell migration assay in the pre-migration stage (upper figure)
 407 and post-migration stage (below figure). At given points in time, images of each condition (n=5) were captured and
 408 free cell area was measured using software analysis. **b**) Cell migration data obtained for cells treated with NO-
 409 loaded ETS-4 and unloaded ETS-4 with a concentration of 90 µg/mL. The migration data of the control without any
 410 material represents 0% and the percentage of wound closure shown for NO-loaded ETS-4 and unloaded ETS-4 is
 411 relative to that value, i.e., the graph only shows the percentage of migration variation between untreated and treated
 412 cells. Data are reported as averages ± standard errors of the averages from three independent assays. Unpaired
 413 student's t-test was used to assess significance with p-values < 0.05 considered statistically significant (*p<0.05). **c**)
 414 Illustrative microscope pictures captured during cell migration assay. The first image on the left, captured without a
 415 detection mask, illustrates the cells (control) in the pre-migration period (t=0 hours). The middle picture, captured
 416 with a detection mask (black area), shows the migration of the control cells after migration time (t= 48 hours). The
 417 first picture from the right, captured with a detection mask, represents the post-migration cells (t= 48 hours) with the
 418 NO-loaded ETS-4 (90 µg/mL), where ETS-4 particles can be noticed.

419

420 Cells were exposed to different concentrations of NO-loaded ETS-4. Results demonstrated that
421 cells treated with a concentration of 90 $\mu\text{g/mL}$ of NO-loaded ETS-4 migrate faster toward the
422 central unseeded region than untreated cells (absence of material); while ETS-4 by itself did not
423 show any statistically significant effect in all time points (Fig. 5 b). After 6 hours of the stoppers
424 removal (when free area starts to be accessible), cells exposed to NO donor displayed an
425 accelerated migration and, consequently, an increased wound closure of $8\pm 1.1\%$ was observed,
426 comparing with the control groups. This significant improvement remained until the end of the
427 experiment. As revealed by comparing the microscope images (Fig. 5 c) of control cells with
428 cells exposed to NO-loaded a ETS-4 the presence of NO greatly increased the closure of the
429 wound after 48 h. Two other concentrations, 180 $\mu\text{g/mL}$ and 45 $\mu\text{g/mL}$, of NO-loaded ETS-4
430 were simultaneously tested (Supplementary Fig. A.10). For the lowest concentration, no
431 differences in the migration rate were observed comparing treated cells and control, while
432 exposing the cells to 180 $\mu\text{g/mL}$, a delay in wound closure was observed. All concentrations
433 were $\leq 180 \mu\text{g/mL}$, the same that exhibited viability above 80% after 72 hours of exposure in
434 the above described HEK_n toxicity tests, thus ensuring no significant toxicity.

435 NO-loaded titanosilicates ETS-10 and ETAS-10 were tested at 450 $\mu\text{g/mL}$ (Supplementary Fig.
436 A.11 A) and B). No improvement in the wound closure was observed. Since these materials
437 present very fast release kinetics, perhaps a higher concentration of material could enhance
438 positive cell responses. However, this was not studied due to the concerns of the toxicological
439 effects of the materials. The synthetic modified clay, CoOS, was also tested at 450 $\mu\text{g/mL}$
440 (Supplementary Fig. A.11 C). In this case, a slight reduction in the cell migration was verified
441 both with NO loaded and unloaded CoOS treatment comparing with control cells without
442 material. For this case, the toxicity effect of this material was evident at this concentration.
443 Using lower concentrations of this material could reduce its toxicological effect and assure a
444 more adequate NO dosage for this application. Yet, its instability (Supplementary Table A.2)
445 would certainly be a limitation, since this causes a fast and uncontrollable NO release that was
446 confirmed by the fast release profile observed in Figure 3 (almost all NO is released within the
447 first 15 minutes).

448 Altogether, these results illustrate the importance of having a slow release of NO to increase cell
449 migration, with fast-releasing compounds being ineffective. It is also important to control the
450 concentration of NO, because NO shows biphasic behavior with stimulatory effects turning into
451 inhibitory effects in a relative narrow range of concentrations.

452

453 **4. Discussion**

454 The evaluation of storage capacity and kinetic release profile, material stability in culture
455 medium and toxicity has demonstrated that not all porous materials that store NO can be
456 considered for biological applications, namely if a fine control of biological functions is
457 envisaged. ETS-4 proved to be the most promising material from those tested, since it is the
458 only one that combines good biocompatibility at 180 $\mu\text{g/mL}$, high stability and controlled NO
459 release, offering thus a great promise to be used in medical applications.

460 ETS-4 loaded with NO was capable of an active regulation of cells O_2 consumption in a
461 reversible way by controlling the NO released amount (*i.e.* material concentration). Moreover,
462 results obtained in Figure 4 clearly show that increasing the amount of NO released, the time of
463 respiration inhibition is longer.

464 Moreover, this new NO donor promoted cell migration and these encouraging results (Fig. 5)
465 clearly highlight the potential application of this material for wound healing. Obviously, the
466 results presented are still far from a clinical demonstration, since they were obtained with an
467 immortalized cell type and with a stagnant media. Nevertheless, this simpler system allows us to
468 get a first assessment of the potentiality of this new NO donor. Additionally, as showed before,
469 sustained NO release was not maintained for 48 hours since ETS-4 is unable to do so and during
470 this time the observed effects can also arise partially from other formed species besides the NO
471 released. Thus, applying multiple doses of NO donor over a certain period may be an option to
472 maintain the optimal therapeutic concentration over time and obtain better results. Nevertheless,
473 NO-based therapy for wounds treatment is challenging due to the high dependence on the
474 specific NO concentration in the affected area: although down-regulation of NO production
475 leads to delayed wound healing by decreasing accumulation of collagen and reducing wound

476 mechanical strength [37,38], overexpression of iNOS, (i.e. excess of NO available in the wound
477 site), may enhance the inflammatory phase of wound healing, leading to keloid lesions [39,40].
478 According to the literature, similar migration tests performed with huESCs cells treated with
479 different concentrations of SNAP (a conventional donor) also confirmed the high dependence of
480 the NO concentration in achieving positive migration responses, demonstrating that depending
481 on the SNAP concentration, treated cells present distinct speed in the migration [41]. Therefore,
482 NO amounts released from ETS-4 at 180 $\mu\text{g/mL}$ and 45 $\mu\text{g/mL}$ are not adequate for this specific
483 application (Supplementary Figure A.10). The same happened with other materials (ETS-10,
484 ETAS-10 and CoOS, Supplementary Figure A.11), which failed in demonstrate capacity to
485 promote cell migration, perhaps not only because of their inadequate NO release profile but also
486 because of other constraints such as the instability in biological medium and toxicity. This
487 underlines the necessity for the more comprehensive evaluation of materials developed in this
488 work that will guide future developments of nanoporous materials for a new therapy approach,
489 with possible application in a broad spectrum of human diseases that would benefit from
490 exogenous NO administration.

491

492 **Acknowledgements**

493 This work was supported by Fundação para a Ciência e Tecnologia (FCT)
494 [IF/00993/2012/CP0172/CT0013 and PTDC/MED-QUI/28721/2017]. This work was developed
495 in the scope of the Projects UID/MULTI/00612/2019 (CQB), UID/ECI/04028/2019 (CERENA)
496 and FCT UID/CTM/50011/2019) (CICECO), financed by Portuguese funds through the
497 FCT/MEC and when applicable co-financed by FEDER under the PT2020 Partnership
498 Agreement.

499 RVP acknowledges for the grant 16/BAD/2017 provided by Colégio de Química, University of
500 Lisbon.

501

502 **Appendix A. Supplementary material**

ACCEPTED MANUSCRIPT

504 **References**

505

- 506 [1] S. Kumar, R.K. Singh, T.R. Bhardwaj, Therapeutic role of nitric oxide as emerging
507 molecule, *Biomed. Pharmacother.* 85 (2017) 182–201.
508 doi:<https://doi.org/10.1016/j.biopha.2016.11.125>.
- 509 [2] M.-M. Cals-Grierson, A.D. Ormerod, Nitric oxide function in the skin, *Nitric Oxide*, 10
510 (2004) 179–193. doi:<https://doi.org/10.1016/j.niox.2004.04.005>.
- 511 [3] R.P. Mason, J.R. Cockcroft, Targeting Nitric Oxide With Drug Therapy, *J. Clin.*
512 *Hypertens.* 8 (2006) 40–52. doi:10.1111/j.1524-6175.2006.06041.x.
- 513 [4] A. Seabra, *Nitric Oxide Donors: Novel Biomedical Applications and Perspectives*,
514 Elsevier Science, 2017. <https://books.google.pt/books?id=iY3fDQAAQBAJ>.
- 515 [5] M.R. Miller, I.L. Megson, Recent developments in nitric oxide donor drugs, *Br. J.*
516 *Pharmacol.* 151 (2007) 305–321. doi:10.1038/sj.bjp.0707224.
- 517 [6] S.T. Gregg, Q. Yuan, R.E. Morris, B. Xiao, Functionalised solids delivering bioactive
518 nitric oxide gas for therapeutic applications, *Mater. Today Commun.* 12 (2017) 95–105.
519 doi:<https://doi.org/10.1016/j.mtcomm.2017.07.007>.
- 520 [7] P.S. Wheatley, A.R. Butler, M.S. Crane, S. Fox, B. Xiao, A.G. Rossi, I.L. Megson, R.E.
521 Morris, NO-releasing zeolites and their antithrombotic properties., *J. Am. Chem. Soc.*
522 128 (2006) 502–509. doi:10.1021/ja0503579.
- 523 [8] M.C. Frost, M.M. Reynolds, M.E. Meyerhoff, Polymers incorporating nitric oxide
524 releasing/generating substances for improved biocompatibility of blood-contacting
525 medical devices, *Biomaterials.* 26 (2005) 1685–1693.
526 doi:<https://doi.org/10.1016/j.biomaterials.2004.06.006>.
- 527 [9] A.C. McKinlay, B. Xiao, D.S. Wragg, P.S. Wheatley, I.L. Megson, R.E. Morris,
528 Exceptional behavior over the whole adsorption-storage-delivery cycle for NO in porous
529 metal organic frameworks., *J. Am. Chem. Soc.* 130 (2008) 10440–10444.
530 doi:10.1021/ja801997r.
- 531 [10] R. V Pinto, F. Antunes, J. Pires, V. Graça, P. Brandão, M.L. Pinto, Vitamin {B3} metal-

- 532 organic frameworks as potential delivery vehicles for therapeutic nitric oxide, *Acta*
533 *Biomater.* 51 (2017) 66–74. doi:<http://dx.doi.org/10.1016/j.actbio.2017.01.039>.
- 534 [11] A.C. Fernandes, F. Antunes, J. Pires, Sepiolite based materials for storage and slow
535 release of nitric oxide, *New J. Chem.* 37 (2013) 4052–4060. doi:10.1039/C3NJ00452J.
- 536 [12] M.L. Pinto, J. Rocha, J.R.B. Gomes, J. Pires, Slow release of NO by microporous
537 titanosilicate ETS-4., *J. Am. Chem. Soc.* 133 (2011) 6396–6402. doi:10.1021/ja200663e.
- 538 [13] M.L. Pinto, A.C. Fernandes, J. Rocha, A. Ferreira, F. Antunes, J. Pires, Microporous
539 titanosilicates Cu²⁺- and Co²⁺-ETS-4 for storage and slow release of therapeutic nitric
540 oxide, *J. Mater. Chem. B.* 2 (2014) 224–230. doi:10.1039/C3TB20929F.
- 541 [14] M.L. Pinto, A.C. Fernandes, F. Antunes, J. Pires, J. Rocha, Storage and delivery of nitric
542 oxide by microporous titanosilicate ETS-10 and Al and Ga substituted analogues,
543 Microporous Mesoporous Mater. 229 (2016) 83–89.
544 doi:10.1016/j.micromeso.2016.04.021.
- 545 [15] A. Fernandes, F. Antunes, M.L. Pinto, J. Pires, Clay based materials for storage and
546 therapeutic release of nitric oxide, *J. Mater. Chem. B.* 1 (2013) 3287–3294.
547 doi:10.1039/c3tb20535e.
- 548 [16] A.C. Fernandes, M.L. Pinto, F. Antunes, J. Pires, Synthetic cobalt clays for the storage
549 and slow release of therapeutic nitric oxide, *RSC Adv.* 6 (2016) 41195–41203.
550 doi:10.1039/C6RA05794B.
- 551 [17] A.C. Fernandes, M.L. Pinto, F. Antunes, J. Pires, L-Histidine-based organoclays for the
552 storage and release of therapeutic nitric oxide, *J. Mater. Chem. B.* 3 (2015) 3556–3563.
553 doi:10.1039/C4TB01913J.
- 554 [18] P.S. Wheatley, A.R. Butler, M.S. Crane, A.G. Rossi, I.L. Megson, R.E. Morris, Zeolites
555 for storage and delivery of nitric oxide in human physiology, in: J. Čejka, N. Žilková, P.
556 Nachtigall (Eds.), *Mol. Sieves From Basic Res. to Ind. Appl.*, Elsevier, 2005: pp. 2033–
557 2040. doi:[https://doi.org/10.1016/S0167-2991\(05\)80570-1](https://doi.org/10.1016/S0167-2991(05)80570-1).
- 558 [19] M. Neidrauer, U.K. Ercan, A. Bhattacharyya, J. Samuels, J. Sedlak, R. Trikha, K.A.
559 Barbee, M.S. Weingarten, S.G. Joshi, Antimicrobial efficacy and wound-healing

- 560 property of a topical ointment containing nitric-oxide-loaded zeolites, *J. Med. Microbiol.*
561 63 (2014) 203–209. doi:10.1099/jmm.0.067322-0.
- 562 [20] C.B. Lopes, P.F. Lito, M. Otero, Z. Lin, J. Rocha, C.M. Silva, E. Pereira, A.C. Duarte,
563 Mercury removal with titanosilicate ETS-4: Batch experiments and modelling,
564 *Microporous Mesoporous Mater.* 115 (2008) 98–105.
565 doi:<https://doi.org/10.1016/j.micromeso.2007.10.055>.
- 566 [21] M.W. Anderson, J. Rocha, Z. Lin, A. Philippou, I. Orion, A. Ferreira, Isomorphous
567 substitution in the microporous titanosilicate ETS-10, *Microporous Mater.* 6 (1996) 195–
568 204. doi:[https://doi.org/10.1016/0927-6513\(95\)00098-4](https://doi.org/10.1016/0927-6513(95)00098-4).
- 569 [22] Z. Lin, J. Rocha, A. Ferreira, M.W. Anderson, Synthesis of microporous titano-alumino-
570 silicate ETAS-10 with different framework aluminum contents, *Colloids Surfaces A*
571 *Physicochem. Eng. Asp.* 179 (2001) 133–138. doi:[https://doi.org/10.1016/S0927-7757\(00\)00648-8](https://doi.org/10.1016/S0927-7757(00)00648-8).
- 572
- 573 [23] J. Rocha, A. Ferreira, Z. Lin, M.W. Anderson, Synthesis of microporous titanosilicate
574 ETS-10 from $TiCl_3$ and TiO_2 : a comprehensive study, *Microporous Mesoporous Mater.*
575 23 (1998) 253–263. doi:[https://doi.org/10.1016/S1387-1811\(98\)00120-6](https://doi.org/10.1016/S1387-1811(98)00120-6).
- 576 [24] N.S. Bryan, M.B. Grisham, Methods to detect nitric oxide and its metabolites in
577 biological samples, *Free Radic. Biol. Med.* 43 (2007) 645–657.
578 doi:<https://doi.org/10.1016/j.freeradbiomed.2007.04.026>.
- 579 [25] V. Georget, V. Baecker, ImageJ-macros: Wound Healing Tool, (n.d.).
580 http://dev.mri.cnrs.fr/projects/imagej-macros/wiki/Wound_Healing_Tool (accessed April
581 1, 2017).
- 582 [26] B.D. Ratner, Chapter 3 - The Biocompatibility of Implant Materials, in: S.F. Badylak
583 (Ed.), *Host Response to Biomater.*, Academic Press, Oxford, 2015: pp. 37–51.
584 doi:<https://doi.org/10.1016/B978-0-12-800196-7.00003-7>.
- 585 [27] B.D. Kevadiya, R.P. Thumbar, M.M. Rajput, S. Rajkumar, H. Bramhatt, G. V. Joshi,
586 G.P. Dangi, H.M. Mody, P.K. Gadhia, H.C. Bajaj, Montmorillonite/poly-(ϵ -
587 caprolactone) composites as versatile layered material: Reservoirs for anticancer drug

- 588 and controlled release property, *Eur. J. Pharm. Sci.* 47 (2012) 265–272.
589 doi:10.1016/j.ejps.2012.04.009.
- 590 [28] M. Ferenc, N. Katir, K. Milowska, M. Bousmina, J.-P. Majoral, M. Bryszewska, A. El
591 Kadib, Haemolytic activity and cellular toxicity of SBA-15-type silicas: elucidating the
592 role of the mesostructure{,} surface functionality and linker length, *J. Mater. Chem. B.* 3
593 (2015) 2714–2724. doi:10.1039/C4TB01901F.
- 594 [29] A.W. Carpenter, M.H. Schoenfisch, Nitric oxide release: Part II. Therapeutic
595 applications, *Chem. Soc. Rev.* 41 (2012) 3742–3752. doi:10.1039/C2CS15273H.
- 596 [30] M. Feelisch, D. Kubitzek, J. Werrigloer, The oxyhemoglobin assay, *Methods Nitric
597 Oxide Res.* (1996) 455–478.
- 598 [31] P.N. Coneski, M.H. Schoenfisch, Nitric oxide release: Part III. Measurement and
599 reporting, *Chem. Soc. Rev.* 41 (2012) 3753–3758. doi:10.1039/C2CS15271A.
- 600 [32] Y.-N. Zhao, X. Xu, N. Wen, R. Song, Q. Meng, Y. Guan, S. Cheng, D. Cao, Y. Dong, J.
601 Qie, K. Liu, Y. Zhang, A Drug Carrier for Sustained Zero-Order Release of Peptide
602 Therapeutics, *Sci. Rep.* 7 (2017) 5524. doi:10.1038/s41598-017-05898-6.
- 603 [33] M.W.J. Cleeter, J.M. Cooper, V.M. Darley-Usmar, S. Moncada, A.H. V Schapira,
604 Reversible inhibition of cytochrome c oxidase, the terminal enzyme of the mitochondrial
605 respiratory chain, by nitric oxide, *FEBS Lett.* 345 (1994) 50–54. doi:10.1016/0014-
606 5793(94)00424-2.
- 607 [34] G.C. Brown, C.E. Cooper, Nanomolar concentrations of nitric oxide reversibly inhibit
608 synaptosomal respiration by competing with oxygen at cytochrome oxidase, *FEBS Lett.*
609 356 (1994) 295–298. doi:10.1016/0014-5793(94)01290-3.
- 610 [35] G.C. Brown, Nitric oxide and mitochondrial respiration, *Biochim. Biophys. Acta -
611 Bioenerg.* 1411 (1999) 351–369. doi:https://doi.org/10.1016/S0005-2728(99)00025-0.
- 612 [36] P. Sarti, M. Arese, A. Bacchi, M.C. Barone, E. Forte, D. Mastronicola, M. Brunori, A.
613 Giuffrè, Nitric Oxide and Mitochondrial Complex IV, *IUBMB Life.* 55 (2003) 605–611.
614 doi:10.1080/15216540310001628726.
- 615 [37] M.R. Schäffer, U. Tantry, S.S. Gross, H.L. Wasserkrug, A. Barbul, Nitric Oxide

- 616 Regulates Wound Healing, *J. Surg. Res.* 63 (1996) 237–240.
617 doi:<https://doi.org/10.1006/jsre.1996.0254>.
- 618 [38] M.R. Schäffer, U. Tantry, F.J. Thornton, A. Barbul, Inhibition of nitric oxide synthesis
619 in wounds: pharmacology and effect on accumulation of collagen in wounds in mice,
620 *Eur. J. Surg.* 165 (1999) 262–267. doi:10.1080/110241599750007153.
- 621 [39] Y.-C. Hsu, M. Hsiao, L.-F. Wang, Y.W. Chien, W.-R. Lee, Nitric oxide produced by
622 iNOS is associated with collagen synthesis in keloid scar formation, *Nitric Oxide*. 14
623 (2006) 327–334. doi:<https://doi.org/10.1016/j.niox.2006.01.006>.
- 624 [40] C.A. Cobbold, J.A. Sherratt, Mathematical Modelling of Nitric Oxide Activity in Wound
625 Healing can explain Keloid and Hypertrophic Scarring, *J. Theor. Biol.* 204 (2000) 257–
626 288. doi:<https://doi.org/10.1006/jtbi.2000.2012>.
- 627 [41] R. Zhan, W. He, F. Wang, Z. Yao, J. Tan, R. Xu, J. Zhou, Y. Wang, H. Li, J. Wu, G.
628 LUO, Nitric oxide promotes epidermal stem cell migration via cGMP-Rho GTPase
629 signalling, *Sci. Rep.* 6 (2016) 30687. doi:10.1038/srep30687.

630

Highlights

- Toxicity, stability and NO release assessed for titanosilicates and clays.
- First validation of these NO donors to regulate biological functions.
- For a positive biological response, low toxicity and slow NO release are required.
- ETS-4 proved to regulate cells' O₂ consumption and accelerate cell migration.
- Application conditions and effect time window are outlined.